Trapping tetracycline-loaded nanoparticles into polycaprolactone fiber networks for periodontal regeneration therapy

WK Wan Abdul Khodir[1], V Guarino[1], MA Alvarez-Perez[1], C Cafiero[2] and L Ambrosio[1]

Abstract

The controlled delivery of antibiotics, anti-inflammatory agents, or chemotherapeutic agents to the periodontal site is a recognized strategy to improve the efficiency of regenerative processes of hard tissues. A novel approach based on the trapping of tetracycline hydrochloride–loaded particles in polycaprolactone nanofibers was used to guide the regeneration processes of periodontal tissue at the gum interface. Chitosan nanoparticles loaded with different levels of tetracycline hydrochloride (up to 5% wt) were prepared by solution nebulization induced by electrical forces (i.e. electrospraying). The fine tuning of process parameters allows to obtain nanoparticles with tailored sizes ranging from 0.485 ± 0.147 µm to 0.639 ± 0.154 µm. The tetracycline hydrochloride release profile had a predominant burst effect for the first 70% of release followed by a relatively slow release over 24 h, which is promising for oral drug delivery. We also demonstrated that trapping tetracycline hydrochloride–loaded particles with submicrometer diameters into a polycaprolactone fiber network contributed to slowing the release of tetracycline hydrochloride from the nanoparticles, thus providing a more prolonged release in the periodontal pocket during clinical therapy. Preliminary studies on human mesenchymal stem cells confirm the viability of cells up to 5 days after culture, and thereby, validate the use of nanoparticle-/nanofiber-integrated systems in periodontal therapies.

[1]Institute of Composite and Biomedical Materials, National Research Council of Italy, Naples, Italy
[2]Department of Dentistry and Maxillo/Facial Surgery, Naples, Italy

Corresponding author:
V Guarino, Institute of Composite and Biomedical Materials, National Research Council of Italy, P.le Tecchio 80, 80125 Naples, Italy.
Email: vguarino@unina.it

Introduction

Periodontal diseases are pathologies affecting the supporting tissues of the teeth. The most common are gingivitis and periodontitis.[1–3] Gingivitis is nondestructive with the formation of gram-positive bacterial *biofilms* (bacterial plaque), which strongly adhere to teeth surfaces.[4] Clinical signs include swelling, spontaneous redness, and bleeding gum tissue after brushing. Periodontitis (chronic and aggressive) is the most common periodontal pathology, affecting up to 70% of the global population, and requiring *restituto in integrum* to preserve the quality of life of the patient. This destructive pathology is mainly caused by gram-negative anaerobic bacteria hosted by the peridontium—that is, gingiva, cementum, alveolar bone, and periodontal ligament. It is the result of a complex bacteria–host response in genetically susceptible patients, in which inflammation stimulates the gingival epithelium to migrate along the tooth surface, so forming the "periodontal pocket." The periodontal pocket provides an ideal site for the growth and proliferation of microorganisms, which cause the loss of connective tissue and progressive breakdown of alveolar bone.[5] In the presence of an intraosseous bone defect, guided tissue regeneration using barrier membranes can be the preferred approach to obtain new periodontal attachment.[6,7] The surgical implantation of periodontal pockets may be associated with infection and inflammation,[8] which can adversely affect the natural progress of tissue regeneration. Controlled delivery of antimicrobials or antibiotics is a promising therapy to prevent and/or treat tissue infection during periodontal surgery,[9] whereas time-controlled release of anti-inflammatory or chemotherapeutic agents in the periodontal site is strongly indicated for improved efficiency of tissue regeneration.[1]

It is extremely important to design carriers able to selectively deliver agents into the periodontal pocket at therapeutic levels[10] to reduce probing depths, more efficiently stabilize tissue interfaces, and minimize bleeding.[9]

Several recent studies focused on the fabrication of chitosan (CHI) nanoparticles by an electrospraying technique to form drug delivery carriers that have interesting preliminary results.[11–13] In particular, the electrospraying process may influence the morphology of polymer particles, just as the electrospinning process has been reported to have an influence on fiber morphology.[14] Electrospraying is compatible with most common drugs used in local delivery, such as tetracycline, doxycycline, minocycline, metronidazole, and chlorhexidine.[9,15,16] Among these, tetracycline hydrochloride (TCH) is the chemical agent most frequently used as an antibiotic in the treatment of periodontal diseases. Clinical studies have shown that TCH has an effective spectrum of activity against many of the anaerobic microbes associated with periodontitis patients.[17] Alternatively, periodontal membranes have been fabricated by including nanosized hydroxyapatite particles as osteoconductive/inductive signals and metronidazole in poly (DL-lactide-*co*-ε-caprolactone) (PLCL) films to fight periodontal pathogens.[17] Here, multilayered electrospun systems composed of protein/polymer ternary blends have recently been developed by coelectrospinning to obtain periodontal barriers for periodontal implants.[17–20]

In this work, we propose a novel approach, based on the simultaneous use of electrospinning and electrospraying techniques, to design integrated membranes that entrap nanoparticles in nanofiber networks for periodontal surgery. Although the idea of using electrospun fibers has been previously investigated for hard tissue applications,[21–27] the novelty of this work lies in the introduction of a reliable and efficient method integrating polymeric carriers in nanofibrous membranes for local drug delivery. In particular, the setup configuration is simple and versatile, requiring the simultaneous injection of solution from two different nozzles. It is possible to control the spatial arrangement of fibers by setting the head motion and collectors. In this work, we propose an integrated system comprising electrospun polycaprolactone (PCL) fibers and TCH-loaded CHI particles—produced *via* electrospraying—to be anatomically adapted at the interface between alveolar

bone and epithelial tissue. It is essential that the integrated periodontal membranes preserve their structural, dimensional, and mechanical integrity long enough to permit periodontal regeneration. The use of PCL ensures the creation of a fiber network with suitable properties in terms of degradability and biocompatibility to meet this prerequisite.[28] The entrapment of TCH-loaded CHI nanoparticles among the nanofibers also provides a controlled release of drug that prevents inflammation in the periodontal pocket.[29]

Materials and methods

Materials

Poly(ε-caprolactone) pellets (PCL; Mn: 45,000 kDa) and CHI (viscosity: 20–300 cP, 1% in 1% acetic acid) were purchased from Sigma–Aldrich (Milan, Italy). Methylene chloride (MC) and methanol were purchased from Sigma–Aldrich for use as solvent and cosolvent in the preparation of PCL solutions. Acetic Acid (pure analytical grade) from JT Baker (Milan, Italy) was used to dissolve CHI. All other chemicals used were analytical grade. TCH was obtained from Sigma–Aldrich and used without any purification.

Fabrication of TCH-loaded CHI particles using electrospraying

CHI powder was dissolved in 90% (v/v) acetic acid solution to form 2% (w/v) CHI solution. CHI solution was gently stirred for 2 days at room temperature until the CHI powder was completely dissolved. TCH—from 1% to 5% w/w with respect to the polymer—was added in 2% (w/v) CHI solution and stirred until complete dissolution of the drug. The TCH-loaded CHI solution has a dark yellow appearance.

The electrospraying process was carried out by using a NANON 01 system (MECC, Japan). Process parameters, that is, voltage, flow rate, and tip/collector distance were varied individually in order to optimize the particle morphology. Aluminum foil was used as a conductive collector plate. All the samples were dried overnight in a fume hood and used for the next step.

Fabrication of integrated particle/fiber membranes

PCL pellets were dissolved in MC/methanol (1:1 v/v) to form a clear and homogenous solution (10% w/v). TCH-loaded CHI solution (2% w/v) with a TCH concentration ranging from 1%–5% w/w with respect to polymer fraction was used for TCH-loaded nanoparticles. Integrated systems were obtained via simultaneous deposition by electrospinning and electrospraying using two separate nozzles in the same spinneret (schematically illustrated in Figure 1) by using the electrospinning equipment. Two different flow rates—0.1 mL/h for TCH-loaded CHI solution and 0.5 mL/h for PCL solution—were used. Moreover, a voltage of 16 kV was imposed at both tips placed at a collector distance of 10 cm. The spinneret, which contains both nozzles, was translationally moved (5 mm/s) along 100 mm width to improve fiber and particle homogeneity. All samples were dried overnight in a fume hood before use.

Morphological studies

The morphology of TCH-loaded CHI particles and integrated membranes—PCL nanofibers with TCH-loaded CHI particles—was investigated by scanning electron microscopy (SEM). The samples were deposited onto gold-coated stubs and analyzed by field emission SEM (Quanta 200 FEI,

The Netherlands). Fiber and particle average diameters were estimated by using Image J software, (version 1.37) on 20 random sample images at the same magnification.

In vitro drug release studies

Encapsulation efficiency and loading capacity of TCH-loaded CHI particles and integrated membranes (PCL nanofibers with CHI particles) were studied. In particular, the amount of free drug released was determined by ultraviolet (UV) spectrophotometry (Cary 100 Varian, Italy). Before UV measurements, samples were centrifuged at 5000 g for 30 min. A linear calibration curve with different concentrations of TCH in phosphate buffer saline (PBS) (pH 7.4) was established to find the correlation between the absorbance and the drug concentration.

TCH-loaded CHI particles and integrated fiber/particle membranes were dipped into 35 mL PBS (pH 7.4) at 37°C ± 0.5°C. Before testing, all the samples were mixed using a vortex for 2–3 min. A portion of the solution (1 mL) was analyzed using a UV visible spectrophotometer at λ_{max} of 380 nm. The detected UV absorbances of TCH were reported in terms of concentration according to the calibration curve of TCH in the buffer. Then, the relative amount of the released TCH was calculated as a function of the incubation time. A graph was plotted for cumulative release of TCH (%) versus time (hours).

The encapsulation efficiency and drug loading were calculated using the following relations:

$$\text{EE (Encapsulation Efficiency)} = (m - m_f)/m$$

where m is the total TCH amount and m_f is the free amount of TCH

$$\text{LC (Loading Capacity)} = m - m_f/m_c$$
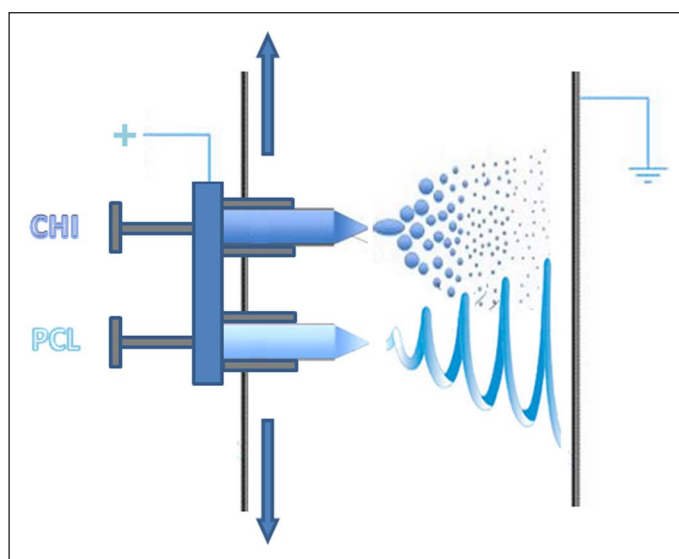
where m_c is the total amount of CHI.

Figure 1. Scheme of the CHI particle trapping procedure by the simultaneous use of electrospinning and electrospraying technique.
CHI: chitosan; PCL: polycaprolactone.

Cell culture

Biological assays were performed using a human mesenchymal stem cell (hMSC) line obtained from Lonza (Milan, Italy). hMSCs were cultured in 75-cm^2 cell culture flasks in Eagle's alpha minimum essential medium (α-MEM) supplemented with 10% fetal bovine serum, antibiotic solution (streptomycin 100 µg/mL and penicillin 100 U/mL; Sigma–Aldrich), and 2 mM L-glutamine. Cells were incubated at 37°C in a humidified atmosphere with 5% CO_2 and 95% air. Four to six passages of hMSCs were used for all the experimental procedures.

Cell morphology

The cell morphology and cell spreading pattern interaction of hMSC cultured onto TCH-loaded CHI particles and integrated PCL/CHI membranes were evaluated by confocal laser scanning microscopy (LSM 510, CarlZeiss). Briefly, hMSCs (1×10^3 cells) were incubated for 24 h, and nonadherent cells were removed by rinsing three times with PBS. Scaffolds were then incubated with CellTracker^{TM} Green CMFDA (5-Chloromethylfluorescein Diacetate) in phenol red–free medium at 37°C for 30 min. Subsequently, the cell culture was washed with PBS and incubated for 1 h in complete medium prior to the LSM visualization.

Cytotoxicity test

To indirectly assess cytotoxicity in hMSC cultures, TCH-loaded CHI particles and integrated PCL/CHI membranes were put onto 24-well cell culture plates in triplicate and incubated after adding 1 mL of α-MEM basal complete media to each well. After 1, 3, and 5 days, media were removed, and 500 µL of the media that was in direct contact with the samples were added into 24-well cell culture plates previously seeded with (1.2×10^4) hMSCs. The hMSC cultures were then removed and washed twice with PBS. A quantity of 500 µL of the media, which was previously in direct contact with the TCH-loaded CHI particles and integrated PCL/CHI membranes, was added to the hMSC cultures. The cell culture plates were further incubated at 37°C, with 5% CO_2 and 95% air humidity, for 1, 3, and 5 days. Indirect cytotoxicity response was validated by the (3-(4,5-dimethylthiazol-2-yl)-2,5-diphenyltetrazolium bromide (MTT) assay. This assay is based on the ability of mitochondrial dehydrogenases of living cells to oxidize a tetrazolium salt (MTT) to an insoluble blue formazan product. The concentration of the blue formazan product is directly proportional to the number of metabolically active cells. The hMSCs were washed with PBS and incubated with fresh culture medium containing 0.5 mg/mL of MTT for 4 h at 37°C in the dark. The supernatant was removed and dimethyl sulfoxide (DMSO) was added. After slow shaking (60 min), the absorbance was quantified by spectrophotometry at 570 nm with a plate reader. The culture medium was renewed every day.

Cell proliferation

The hMSCs (1.6×10^4 cells) were plated onto TCH-loaded CHI particles and PCL-/CHI-integrated membranes. Cell proliferation was evaluated by the Alamar Blue assay (AbD Serotec Ltd, UK) for 7, 14, and 21 days of culture. This assay allows quantification of the fluorescence of the product formed from reduction by mitochondrial enzymes such as flavin mononucleotide dehydrogenase, flavin adenine dinucleotide dehydrogenase, and nicotinamide adenine dinucleotide dehydrogenase. Redox product levels also gave quantitative indications about metabolic activity of living cells. Alamar Blue (1 mL) was diluted in phenol red–free medium (1:10) according to the manufacturer's protocol, and cells were incubated for 4 h at 37°C, with 5% CO_2. Afterward, the solution

(100 μL) was transferred into a 96-well plate for colorimetric analyses. Cell-free plates were used to correct any background interference from the redox indicator. The optical density was immediately measured by a spectrophotometer (Sunrise; Tecan, Männedorf, Zurich, Switzerland) at wavelengths of 540 and 600 nm.

Statistical analysis

All numerical data are presented as mean ± standard deviation. All results were subjected to statistical evaluation using an unpaired Student's t-test to determine significant differences between groups. The significance level was set at $p < 0.05$.

Results and discussion

TCH-loaded CHI particles

Electrospraying was used to produce nanoparticles. The charge and size of the particles were controlled to some extent by electrical forces—that is, by adjusting flow rate and voltage applied to the nozzle.[30] According to Arya et al.,[11] spherical CHI particles have been prepared using 90% (v/v) acetic acid solution, which provided optimal viscosity for jet breaking induced by electrical forces. This arises from the particular effects of acetic acid concentration on the conductivity[13] and surface tension.[31] The low degree of dissociation of acetic acid ensures moderate conductivity and viscosity properties that enhance the stabilization of the electrospraying process.

In this study, the feasibility of preparing TCH-loaded CHI particles by electrospraying was investigated at different levels of TCH. The relative TCH amount affects the morphology and the average size of CHI particles, as reported in Figure 2. By loading in 1% w/w TCH, the CHI formed a monodisperse distribution of clustered particles with an average individual diameter of 803 ± 128 nm (Figure 2(e)). As the TCH loading increased to 3% and 5% w/w, a more heterogeneous distribution of particle sizes and a decrease in particle diameters was observed. The use of nanosized particles with high surface area generally promoted a uniform release of the encapsulated drug, which made them useful for mucosal or nasal delivery. In addition, confirmed by several studies, the suitability of CHI as a drug carrier has been demonstrated by its excellent mucoadhesive properties.[32]

The biodegradable properties of CHI-based systems enable highly tunable drug release for treatment of different diseases as a function of specific drugs and polymer formulations.[15] However, the use of different microencapsulation techniques may influence the kinetics of drug release from micro-/nanoparticles.[8,10,29] Therefore, we used electrically assisted techniques to prepare TCH-loaded CHI micro-/nanoparticles for short-term TCH release, as shown in Figure 3. The TCH release curve has a rapid initial burst during the first 3 h, followed by a prolonged drug release that occurs during the next 4 h. Also, the release rate increased as the concentration of TCH increased.

Antibiotic release is primarily driven by the fluid diffusion through the particle matrix. In this case, rapid dissolution of particles produces a kinetic profile with a large initial burst region. This is a positive attribute, in that the initial burst release is often required to achieve a sufficient initial dosage capable of eliminating intruding bacteria before they begin to proliferate.[33] This burst release was ascribable to a preferential drug distribution on the particle surface. The TCH diffused easily during the first stage of the incubation, supported by the fast degradation of CHI particles as reported previously.[34] The drug dissolution was also facilitated by the hydrophilic nature of CHI, which allowed rapid penetration of water into the particles. While the
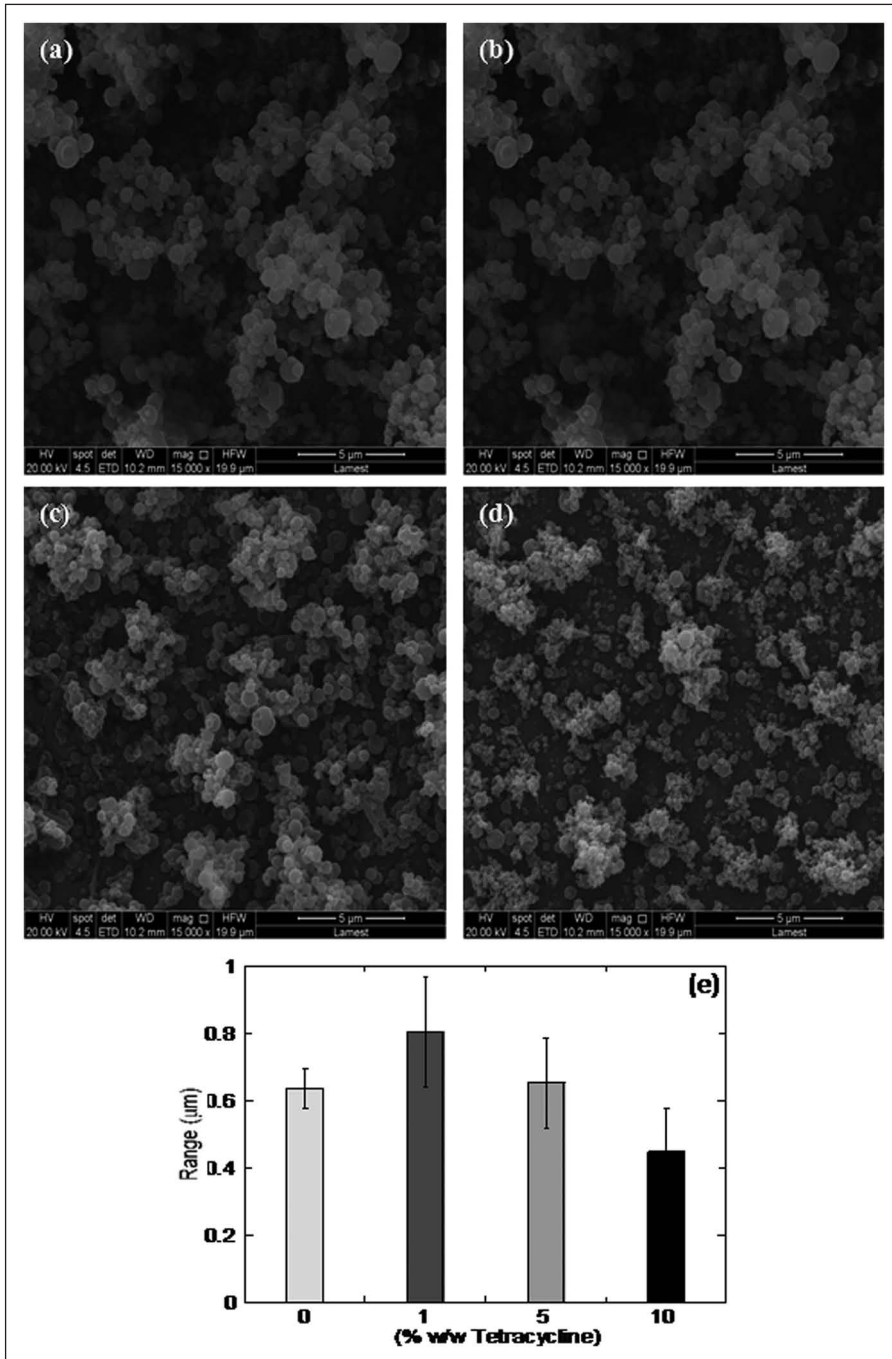
Figure 2. TCH-loaded CHI nanoparticles via electrospraying techniques: (a–d) SEM images of particles with different TCH loading; (a) 0%, (b) 1%, (c) 3%, and (d) 5% w/w (magnification 15kx, scale bar = 5 μm) and (e) particle size average diameter versus % (w/w) TCH concentration by image analysis.
TCH: tetracycline hydrochloride; CHI: chitosan.

encapsulation efficiency and drug loading are invariant with TCH concentration, the drug release rate seemed to be dependent upon the relative amount of TCH used (Figure 3). Indeed, the 1%, 3%, and 5% w/w TCH-loaded CHI particles had a high encapsulation efficiency of 97.8%, 98.1%, and 98.0%, respectively. The measured drug amount was approximately 0.97%, 2.9%, and 4.9% for 1%, 3%, and 5% w/w fractions, respectively. At higher TCH concentrations, the hydrophilic nature of TCH and its high water solubility tend to promote the formation of molecular clusters that were not physically bound to the polymer but were entrapped in the polymer network.[34,35] Consequently, TCH-loaded particles with higher drug concentration had faster drug release.

The fluorescent images obtained by confocal microscopy of TCH-loaded CHI micro-/nanoparticles with cells are presented in Figure 4. The green staining indicated that hMSCs were vital to the direct contact of TCH with independent CHI particles on TCH loading (Figure 4(a) to (d)). In particular, an improved cell growth is apparent in the case of 1% TCH CHI particles, where spindle-like cell shapes were detected with extended and aligned filopodia. In contrast, the cells spread without any orientation preference in the case of CHI particles with 5% TCH. This evidence is supported by the indirect MTT and Alamar Blue reduction tests (Figure 5(a) and (b)) for samples with different TCH loading. After 1, 3, and 5 days of hMSC exposure to the eluent, the cell activity was progressively reduced with increased amounts of TCH, indicating a cytotoxic effect of TCH.

TCH-loaded CHI particles and PCL nanofiber–integrated membranes

The development of integrated fiber/particle systems opens an interesting route to fabricate membranes with tunable physico-chemical, mechanical, and biological properties that could lead to more efficacious periodontal regeneration. The electrospinning and electrospraying technique used simultaneously to produce nonwoven PCL fibers can entrap TCH-loaded CHI particles
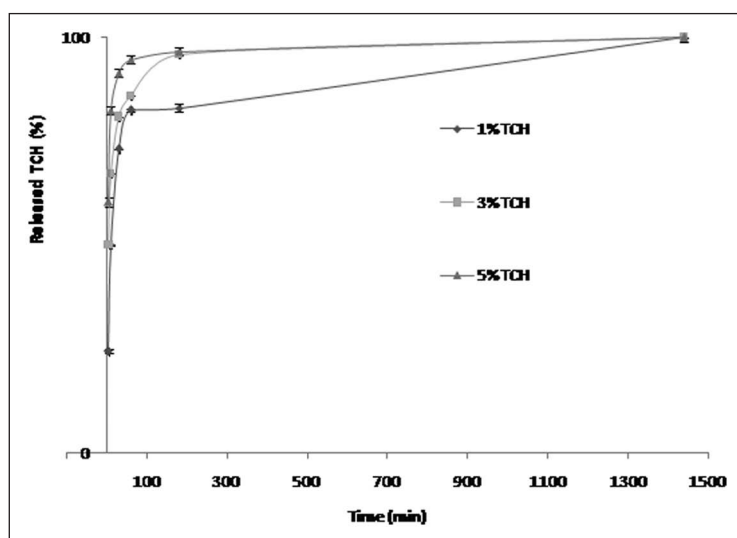

Figure 3. TCH release profiles from CHI particles with different TCH loading at 37°C.
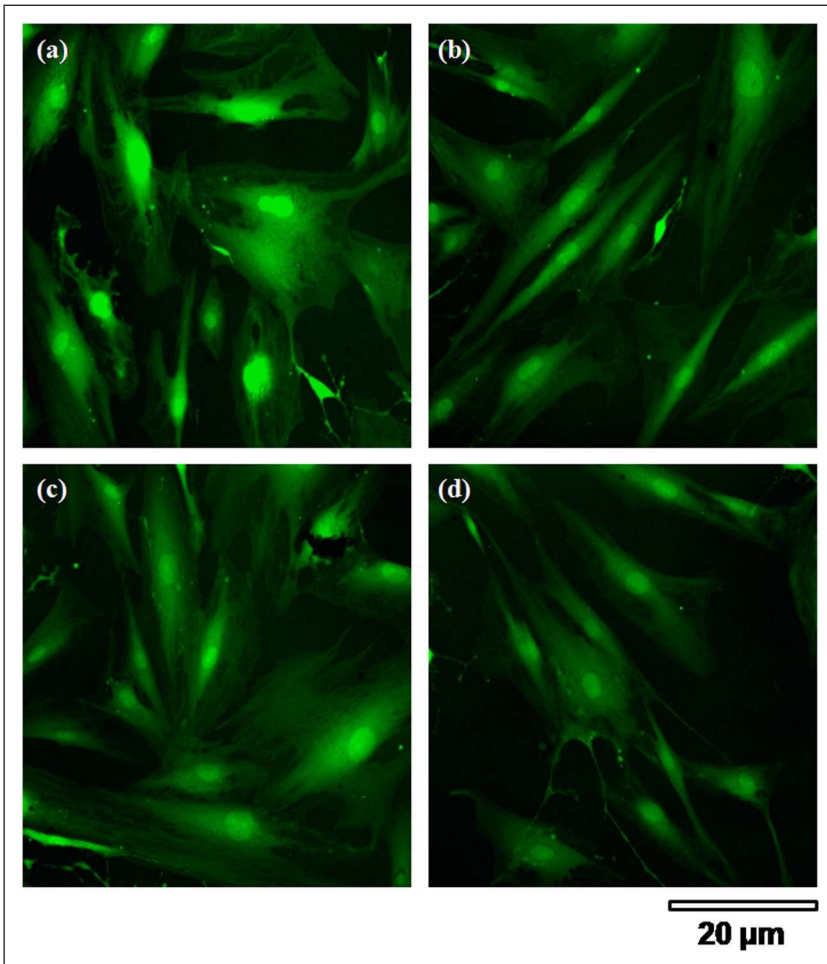TCH: tetracycline hydrochloride: CHI: chitosan.

Figure 4. Biocompatibility of TCH-loaded CHI particles: confocal images of CHI particles with different TCH loading—(a) 0%, (b) 1%, (c) 3%, and (d) 5% (w/w).
TCH: tetracycline hydrochloride; CHI: chitosan.

(Figure 6). The setup requires the use of two different nozzles, working at the same voltage but different flow rates.

Moving the head spinneret during spinning (at approximately 5 mm/s) has also been used to balance the evaporation phenomena, which occurs during simultaneous spinning. This motion promotes solvent evaporation from PCL solution due to higher MC volatility. The MC volatility also promotes surface roughening of PCL fibers. In contrast, the acetic acid evaporation does not occur completely, but solvent traces still reside in CHI particles before their deposition. This promotes chemical anchorage of the particles on the PCL fiber surface (Figure 6), which could be relevant for the prevention of any transmembrane crossing of CHI particles during in vitro culture, thus affecting specific cell activities.[36]

The effect of the process parameters, such as voltage and flow rate, was investigated with the aim of optimizing fiber and particle morphology. Image analysis data for PCL/CHI membranes produced at three different voltages (14, 16, and 17 kV) and constant flow rate (0.3
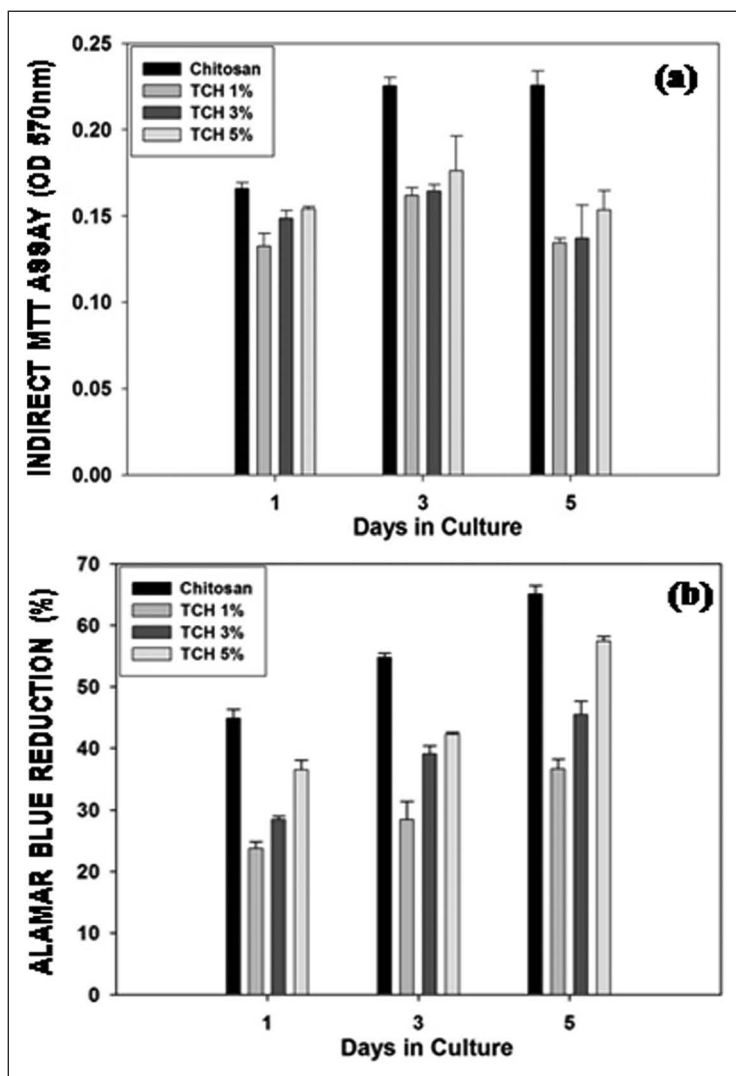
Figure 5. (a) MTT assay and (b) Alamar Blue reduction versus time of culture of TCH-loaded CHI particles.
MTT: (3-(4,5-dimethylthiazol-2-yl)-2,5-diphenyltetrazolium bromide; TCH: tetracycline hydrochloride; CHI: chitosan.

mL/h) are presented in Figure 7(a). The PCL fibers and CHI particles had comparable average diameters—0.601 μm and 0.642 μm, respectively—at the lowest applied voltage (14 kV). The increase of voltage up to 17 kV increased the particle size to 0.680 μm. Notably, an increased voltage also promoted jet instability, resulting in a wide fiber diameter distribution, from 0.549 to 0.788 μm,[14] as voltage increased. A comparison of PCL/CHI membranes prepared at different flow rates is presented in Figure 7(b). PCL fibers show a slight reduction of fiber diameter from 0.567 to 0.491 μm as the flow rate decreases from 0.1 to 0.3 mL/h. Similarly, TCH-loaded CHI particles show a greater reduction in size from 0.712 to 0.519 μm. Notably, a decrease in CHI particle population on the surface of PCL fibers is detected as the voltage and flow rate increase. This indicated
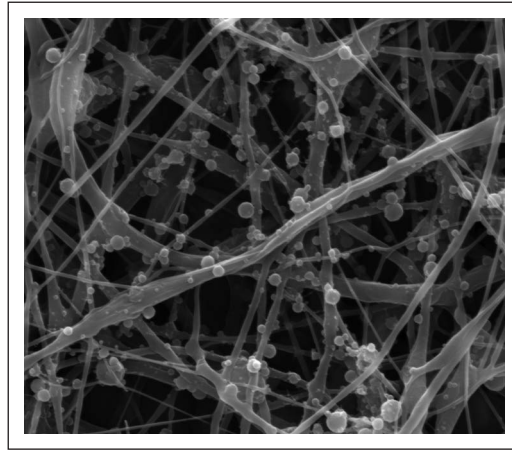
Figure 6. SEM (magnification 20 k×, scale bar = 5 μm) of TCH-loaded (3% w/w) CHI particles trapped in PCL fibers by simultaneous electrospraying/electrospinning technique.
SEM: scanning electron microscopy; CHI: chitosan; PCL: polycaprolactone; TCH: tetracycline hydrochloride.
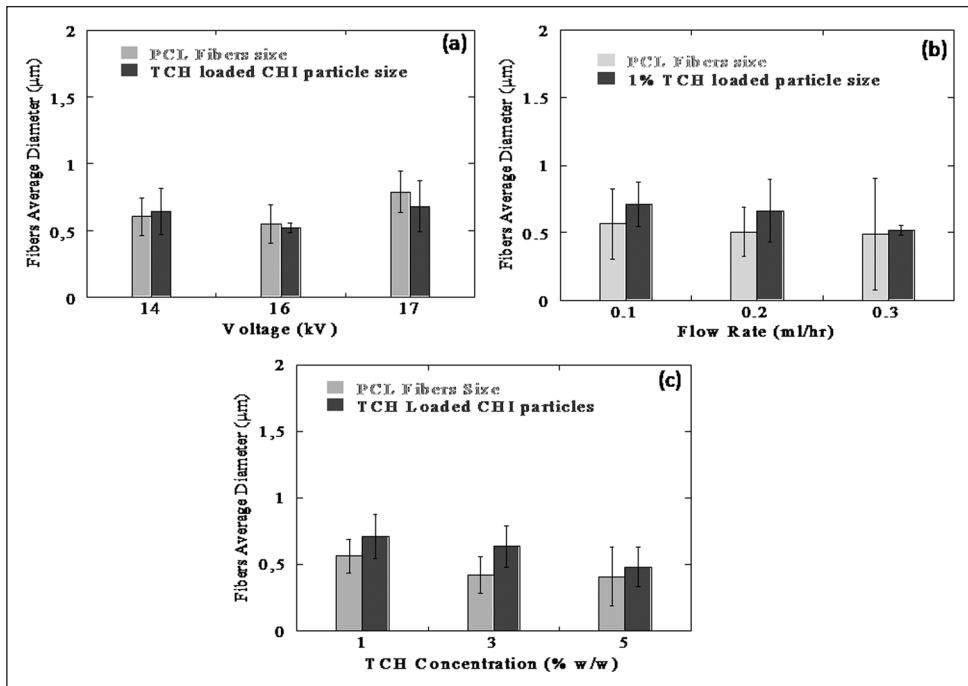

Figure 7. Image analysis of PCL fibers and TCH-loaded CHI particles. Estimation of the characteristic diameter as a function of (a) voltage, (b) flow rate, and (c) TCH-loading amount.
CHI: chitosan; PCL: polycaprolactone; TCH: tetracycline hydrochloride.

that the simultaneous deposition of particles with PCL fibers may affect CHI particle formation, as confirmed by the presence of fewer particles and associated spatial heterogeneity.

The effect of TCH concentration on the final morphology of CHI particles is shown in Figure 7(c). Monodispersed particles with average size of 0.712 μm are obtained in the case of 1% w/w TCH. As the TCH concentration rises up to 5% w/w, TCH-loaded CHI particle size decreases down to 0.485 μm. These data indicated a higher tendency of TCH to form clusters at high concentrations, which favors the interaction among CHI chains during particle formation.

TCH release from integrated PCL/CHI membranes was studied to evaluate the role of the surrounding fibrous network on the release of drug from nanoparticles. For all the samples tested, full encapsulation efficiency (approximately 100%) was calculated, independent of TCH content, as required in controlled drug release studies. The release profiles of CHI particles and PCL/CHI membranes containing 1%, 3%, and 5% w/w TCH are reported in Figure 8.

All the profiles have an initial burst release during the first 30 min, followed by a prolonged release in agreement with release profiles of CHI particles as shown in the case of CHI particles alone (Figure 3). Comparative analysis of the release mechanisms revealed slower release kinetics from CHI particles within a fibrous PCL network. This suggests a "retention effect" offered by the PCL nanofiber network on the release of highly hydrophilic TCH molecules. From observations of TCH release from CHI particles, the profile of integrated membranes had an increase in the burst effect (Figure 8), from 17% to 58% of the total released amount as the TCH concentration increases. The sustained release is preferentially due to the effect of nanoparticle size and shape on the depletion of the drug content, both affecting the diffusion of medium into particles and of TCH from the core to the surface.[37] However, a slowing of the TCH release was detected in the case of trapped CHI particles versus CHI particles alone. This would provide more controlled release of drug in the periodontal pockets, where the pharmaceutical dose is crucial.[8,38]

The biological response of the TCH-loaded PCL/CHI fibers was investigated as a preliminary stage in their validation for clinical use. The hMSCs were evaluated in terms of cell morphology, growth, and phenotypic expression after in vitro culture. Confocal images of CHI/PCL fibers with different TCH loading are presented in Figure 9(a) to (e), with PCL nanofibers used as a control. Green staining is detected for all the TCH-loaded CHI/PCL fibers, indicating a higher number of vital cells in the presence of trapped CHI particles independent of TCH content.

Quantitative analyses (Figure 10(a) and (b)) confirm the high viability of hMSCs up to 5 days of culture. In particular, MTT tests and Alamar Blue reduction show a progressive decrease of cell proliferation during the first 5 days of culture, which confirms the negative effect of the higher TCH concentrations on cell response (Figure 10(b)). Based on hMSC biocompatibility results, TCH drug carried by CHI nanoparticles provided chemical signals that did not deleteriously affect cell activity, while the entrapment of CHI nanoparticles in PCL fibers promoted a more homogeneous and efficient distribution of the molecular signals to cells.

Conclusion

The inclusion of particles in the fiber network provided better distribution of drug into the scaffolds, due to the homogeneous distribution of the particles, and extended the release time of TCH, due to the effect of hydrophobic PCL fibers. Trapping the TCH-loaded CHI nanoparticles in PCL electrospun membranes was effected by simultaneous use of electrospinning and electrospraying techniques. The dual nozzle system assured a homogeneous distribution of the CHI particles among PCL fibers. Good attachment and cell proliferation of hMSCs were observed; however, our studies showed hMSC cytotoxicity related to the higher TCH concentrations. These preliminary results are promising and encourage the future use of TCH-loaded CHI
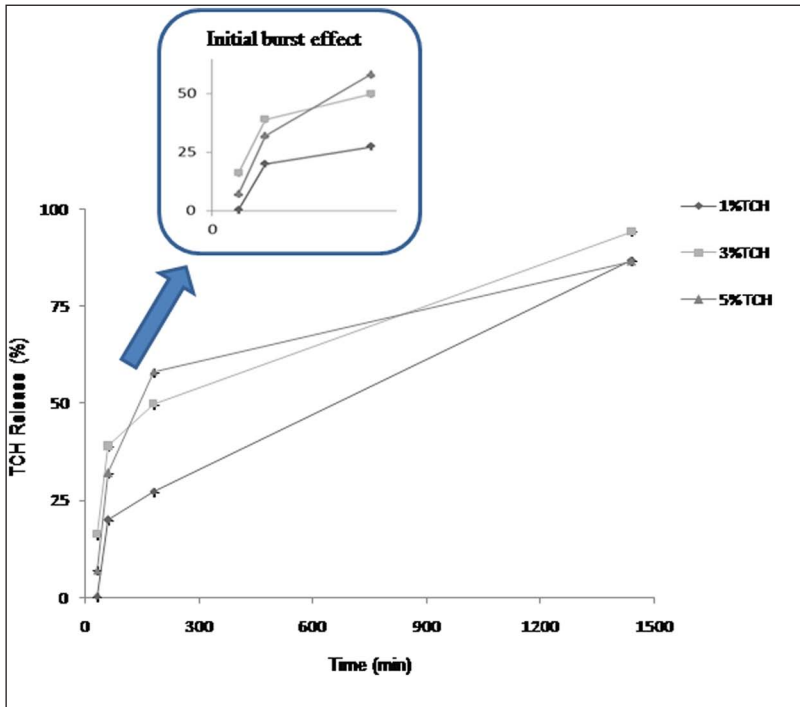
Figure 8. TCH release profiles from PCL/CHI membranes with different TCH release profiles at 37°C.
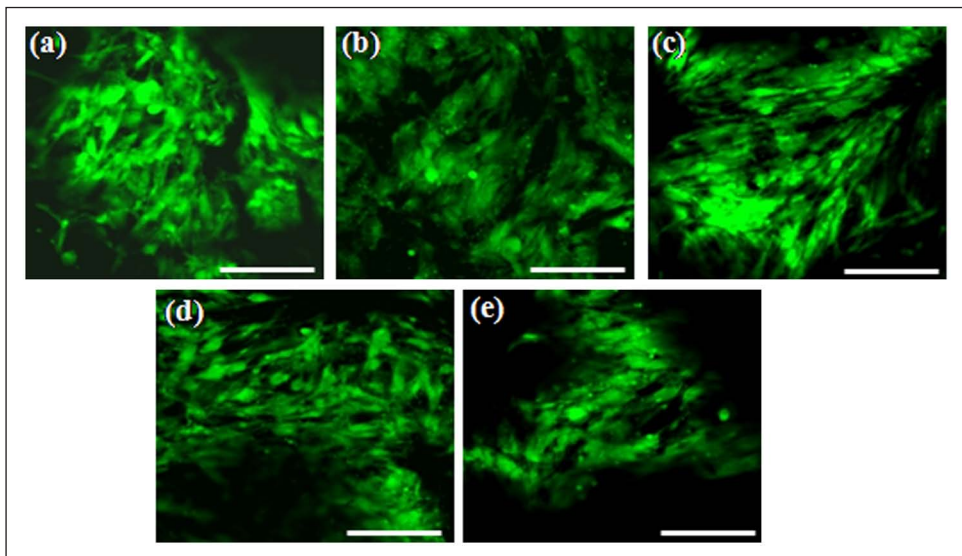CHI: chitosan; PCL: polycaprolactone; TCH: tetracycline hydrochloride.

Figure 9. hMSC response of TCH-loaded PCL/CHI membranes: (a–c) confocal images of membranes with different TCH loading—(a) 0%, (b) 1%, (c) 3%, and (d) 5% (w/w) and (e) PCL nanofiber control (scale bar = 50 µm).
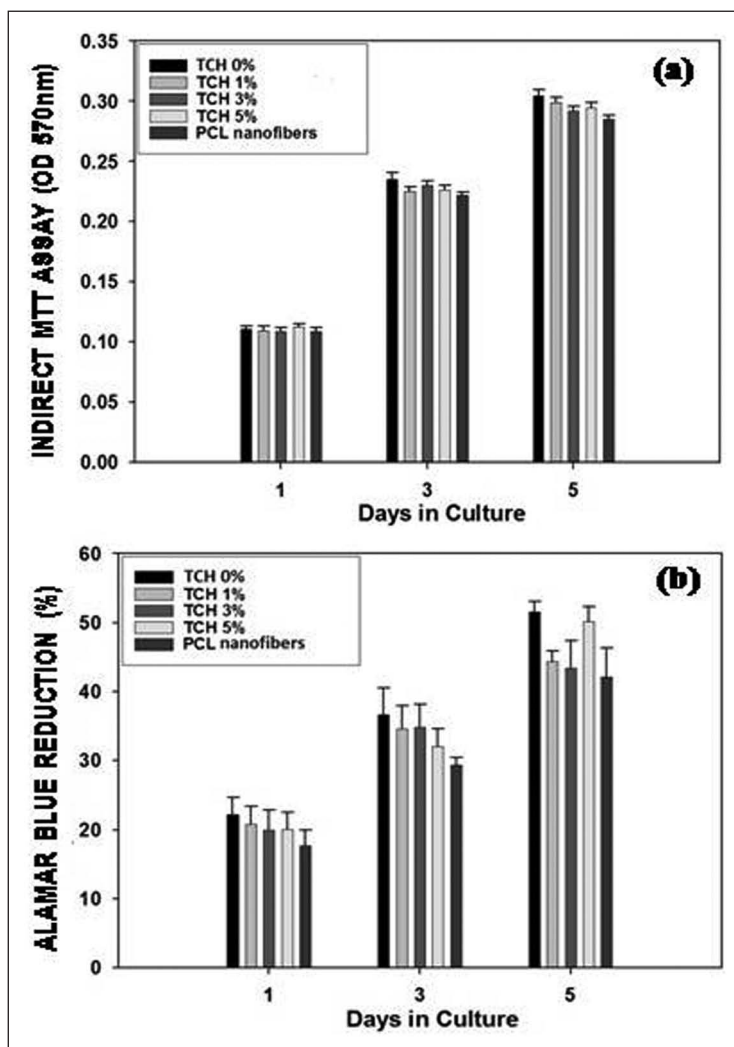hMSC: human mesenchymal stem cell; CHI: chitosan; PCL: polycaprolactone; TCH: tetracycline hydrochloride.

Figure 10. (a) MTT assay (b) and Alamar Blue reduction during 1, 3, and 5 days of culture.
MTT: (3-(4,5-dimethylthiazol-2-yl)-2,5-diphenyltetrazolium bromide; OD: optical density.

particles entrapped in PCL fibers for in vivo studies in human periodontal pockets. This would establish the efficacy of this technology as a minimally invasive approach suitable to proceed to clinical trials.

References

1. Jernberg GR. European Patent Specification EP 0 528 998 B1, 1997.

2. Niemic BA. Periodontal disease. *Top Companion Anim Med* 2008; 23(2): 72–80.

3. Armitage GC. Development of a classification system for periodontal diseases and conditions. *Ann Periodontol* 1999; 4(1): 1–6.

4. Socransky SS. Microbiology of periodontal disease—present status and future considerations. *J Periodontol* 1977; 48(9): 497–504.

5. Lindhe J, Lang NP and Kerring T. *Clinical periodontology and implant dentistry*. 5th ed. Wiley-Blackwell, 2008, pp. 734–766.

6. Gottlow J, Nyman S, Karring T, et al. New attachment formation as the result of controlled tissue regeneration. *J Clin Periodontol* 1984; 11: 494–503.

7. Cortellini G, Pini Prato G and Tonetti M. Periodontal regeneration of human intrabony defects with bioresorbable membranes. A controlled clinical trial. *J Periodontol* 1996; 67: 217–223.

8. Pragati S, Ashok S and Kuldeep S. Recent advances in periodontal drug delivery system. *Int J Drug Deliv* 2009; 1: 1–14.

9. Divya PV and Nandakumar K. Local drug delivery—periocol in periodontics. *Trends Biomater Artif Organs* 2006; 19(2): 74–80.

10. Kumari A, Yadav SK and Yadav SC. Biodegradable polymeric nanoparticles based drug delivery systems. *Colloids Surf B Biointerfaces* 2010; 75(1): 1–18.

11. Arya N, Chakraborty S, Dube N, et al. Electrospraying: a facile technique for synthesis of chitosan-based micro/nanospheres for drug delivery applications. *J Biomed Mater Res B Appl Biomater* 2009; 88: 17–31.

12. Songsurang K, Praphairaksit N, Siraleartmukul K, et al. Electrospray fabrication of doxorubicin-chitosan-tripolyphosphate nanoparticles for delivery of doxorubicin. *Arch Pharm Res* 2011; 34(4): 583–592.

13. Zhang S and Kawakami K. One-step preparation of chitosan solid nanoparticles by electrospray deposition. *Int J Pharm* 2010; 397(1–2): 211–217.

14. Guarino V, Cirillo V, Alvarez-Perez MA, et al. Tuning size scale and crystallinity of PCL electrospun fibres via solvent permittivity to address hMSC response. *Macromol Biosci* 2011; 11(12): 1694–1705.

15. Palmer RM, Watts TLP and Wilson RF. A double-blind trial of tetracycline in the management of early onset periodontitis. *J Clin Periodontol* 1996; 23(7): 670–674.

16. Dumitrescu AL. *Antibiotics and antiseptics in periodontal therapy*. Berlin, Heidelberg: Springer-Verlag, 2011.

17. Bottino MC, Thomas V and Janowski GM. A novel spatially designed and functionally graded electrospun membrane for periodontal regeneration. *Acta Biomater* 2011; 7: 216–224.

18. Yazhou W, Bochu W, Weili Q, et al. A novel controlled release drug delivery system for multiple drugs based on electrospun nanofibers containing nanoparticles. *J Pharm Sci* 2010; 99(12): 4805–4811.

19. Gupta D, Venugopal J, Mitra S, et al. Nanostructured biocomposite substrates by electrospinning and electrospraying for the mineralization of osteoblasts. *Biomaterials* 2009; 30(11): 2085–2094.

20. Jaworek A, Krupa A, Lackowski M, et al. Nanocomposite fabric formation by electrospinning and electrospraying technologies. *J Electrostat* 2009; 67(2–3): 435–438.

21. Francis L, Venugopal J, Prabhakaran MP, et al. Simultaneous electrospin-electrosprayed biocomposite nanofibrous scaffolds for bone tissue regeneration. *Acta Biomater* 2010; 6(10): 4100–4109.

22. Zhang H. Effects of electrospinning parameters on morphology and diameter of electrospun PLGA/MWNTs fibers and cytocompatibility in vitro. *J Bioact Compat Polym* 2011; 26(6): 590–606.

23. Lu H, Chen WJ, Xing Y, et al. Design and preparation of an electrospun biomaterial surgical patch. *J Bioact Compat Polym* 2009; 24: 158–168.

24. Zamani M, Morshed M, Varshosaz J, et al. Controlled release of metronidazole benzoate from poly ε-caprolactone electrospun nanofibers for periodontal diseases. *Eur J Pharm Biopharm* 2010; 75: 179–185.

25. Wang P, Gong P, Lin Y, et al. Nanofibrous electrospun barrier membrane promotes osteogenic differentiation of human mesenchymal stem cells. *J Bioact Compat Polym* 2011; 26: 607–618.

26. Prabaharan M, Jayakumar R and Nair SV. Electrospun nanofibrous scaffolds-current status and prospects in drug delivery. *Adv Polym Sci* 2012; 246: 241–262.

27. Guarino V, Alvarez-Perez MA, Cirillo V, et al. hMSC interaction with PCL and PCL/gelatin platforms: a comparative study on films and electrospun membranes. *J Bioact Compat Polym* 2011; 26(2): 144–160.

28. Andrady AL. *Science and technology of polymer nanofibers*. Hoboken, NJ, USA: John Wiley & Sons, Inc., 2008.

29. Govender S, Lutchman D, Pillay V, et al. Enhancing drug incorporation into tetracycline-loaded chitosan microspheres for periodontal therapy. *J Microencapsul* 2006; 23(7): 750–761.

30. Jaworek A and Sobczyk AT. Electrospraying route to nanotechnology: an overview. *J Electrostat* 2008; 66(3–4): 197–219.

31. Geng X, Kwon O and Jang J. Electrospinning of chitosan dissolved in concentrated acetic acid solution. *Biomaterials* 2005; 26: 5427–5432.

32. Park JH, Ye M and Park K. Biodegradable polymers for microencapsulation of drugs. *Molecules* 2005; 10: 146–161.

33. Xu X, Zhong W, Zhou S, et al. Electrospun PEG—PLA nanofibrous membrane for sustained release of hydrophilic antibiotics. *J Appl Polym Sci* 2010; 118: 588–595.

34. Rane YM, Mashru RC, Sankalia MG, et al. Investigations on factors affecting chitosan for dissolution enhancement of oxcarbazepine by spray dried microcrystal formulation with an experimental design approach. *Drug Dev Ind Pharm* 2007; 33(9): 1008–1023.

35. Govender T, Riley T, Ehtezazi T, et al. Defining the drug incorporation properties of PLA—PEG nanoparticles. *Int J Pharm* 2000; 199: 95–110.

36. Singla AK, Sharma ML and Dhawan S. Chitosan: some pharmaceutical and biological aspects—an update. *Biotech Histochem* 2001; 76: 165–171.

37. Guarnieri D, Guaccio A, Fusco S, et al. Effect of serum proteins on polystyrene nanoparticle uptake and intracellular trafficking in endothelial cells. *J Nanopart Res* 2011; 13(9): 4295–4309.

38. Sendil D, Gürsel I, Wise DL, et al. Antibiotic release from biodegradable PHBV microparticles. *J Control Release* 1999; 59(2): 207–217.